STANFORD UNIVERSITY
DEPARTMENT OF ELECTRICAL ENGINEERING
STANFORD ELECTRONICS LABORATORIES

FINAL TECHNICAL REPORT

BIOELECTRIC SIGNAL ANALYSIS AND MEASUREMENT

Principal Investigator

David C. Lai

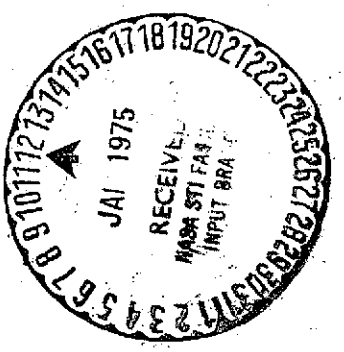

January 1975

Prepared under
Grant NGR 05-020-575
for
Ames Research Center
National Aeronautics and Space Administration

BIOELECTRIC SIGNAL ANALYSIS AND MEASUREMENT

The goals of this research project are: (a) to use nonstationary time-series techniques to analyze EEG signals for the estimation of alertness; (b) to extract time-varying order in sequential time-series measurement of these data; and (c) to devise strategies for obtaining optimal representation of the EEG signal. Significant accomplishments on each of these goals have been made. Most of the results have been presented in various international and national scientific conferences and published in the open literature. This report will mainly consist of reprints of these published papers. However, we shall give a brief account of our accomplishments as follows.

(1) We have successfully implemented a frequency-discrimination technique for EEG to obtain the rate of change of its phase. This is based on the model that EEG is a phase and amplitude modulated signal with carrier frequency center around the α-rhythm, viz.,

$$e(t) = a(t) \cos \left[2\pi f_{\alpha} t + \phi(t) \right]$$

where $a(t)$ represents the slow amplitude variation of the signal; $\phi(t)$ represents the phase variation of the signal; and f_{α} designates the α-rhythm frequency which is about 8 - 13 Hz. Details are reported in a paper published in the Proceedings of the 1972 National Electronics Conference.

(2) A mathematical model for the photically stimulated EEG signals has

been conceived and simulated, based on the phase alignment of EEG signals with the photic stimulus. In the model, a parameter b which represents the speed of the propagation of the phase uncertainty is thought to be related to the alertness states. Calibration of this parameter with respect to the alertness stages would make this parameter a useful tool for alertness estimate. Details of this model are described in a paper entitled "A Model for the Photically Stimulated Electroencephalographic Signals", published in the Proceedings of the 12th Annual San Diego Biomedical Symposium.

(3) Spectral analysis of EEG signals has been used for many years. However, real time hard copy displays of the time-varying power spectrum that permit tracking of dynamic brain states have been lacking. A scheme was implemented. This scheme enables us to obtain a display with the amplitude being exhibited both in waveform and in gray intensity. Visually, this hard copy produces a three-dimensional effect. The display shows clearly the dynamic changes in the power spectrum of the EEG. The detailed description of this program dubbed "GIFBUF" written by F. Mansfield was submitted earlier.

(4) The representation of EEG signals has always been a major problem in the automatic analysis of EEG signals. We have developed a representation for EEG signals and their in-phase and quadrature components. This representation makes easy the monitoring and tracking of EEG frequencies and phases. The development and implementation of this representation resulted in two papers: "Real-time EEG Analysis and Monitoring Using

In-phase and Quadrature Components", published in the Proceedings of the 26th Annual Conference on Engineering in Medicine and Biology, and "Error-free Representation of EEG Signals", published in the Proceedings of the 1973 IEEE International Conference on Systems, Man and Cybernetics.

(5) It has been a major task to separate signal from noise in EEG analysis. We devised a scheme by modeling an EEG signal in the form of a sinusoid waveform and an additive noise which represents the incoherent component of the signal. With this model, we developed a scheme which will estimate the signal-to-noise ratio in the most commonly used processing situation; viz., averaging. The technique and results are described in "Estimating Signal and Noise in Coherent Time Averages of EEG Data", published in the Proceedings of the 26th Annual Conference on Engineering in Medicine and Biology.

(6) A nonlinear oscillator model for EEG signals has been developed. This model has proven to encompass many reported phenomena and predicted several unreported phenomena when the subjects were under periodic photic stimulation. The oscillator used is the van der Pol oscillator described by:

$$\ddot{x} - \mu\left(1 - x^2\right)\dot{x} + \omega_0^2 x = \omega_0^2 e(t)$$

where $x(t)$ denotes the EEG signal to be modeled; ω_0 is the autonomous alpha frequency; $e(t)$ is the external stimulus; and μ is the coupling coefficient. This model also elucidates the effect of a stimulus flash to the phase of an EEG signal. The details are reported in a paper, "A Nonlinear Model of EEG Entrainment by Periodic Photic Stimulation",

published in the Proceedings of the 7th Annual Conference of the Neuroelectric Society.

(7) To monitor or track the alertness states via EEG signals, we need the ability to predict the EEG waveforsm. For this purpose, we used an autoregressive process representation. This endeavor resulted in a paper entitled, "Prediction of EEG Waveforms by Using an Autoregressive Model", to be presented at the 1975 San Deigo Biomedical Symposium. The full paper will be published in the Proceedings. A reprint of the abstract of this paper is attached.

In summary, we have accomplished most of the objectives as proposed.

APPLICATION OF FREQUENCY DISCRIMINATION TECHNIQUE TO THE ANALYSIS OF ELECTROENCEPHALOGRAPHIC SIGNALS

D. C. Lai
Stanford University
Department of Electrical Engineering
Stanford, California 94305

R. L. Lux
University of Utah Medical Center
Cardiology Division
Salt Lake City, Utah 84112

Reprinted from the Proceedings of the National Electronics Conference, vol. 27, pp. 80-85, October 1972.

A portion of this work was carried out at the Department of Electrical Engineering, the University of Vermont, Burlington, Vermont, and was supported in part by NASA Grant NGR 46-001-038. At Stanford University, it was also supported in part by NASA Grant NGR 05-020-575 from NASA-Ames Research Center and ARPA Contract DAHC15-72-C-0232.

APPLICATION OF FREQUENCY DISCRIMINATION TECHNIQUE TO THE ANALYSIS OF ELECTROENCEPHALOGRAPHIC SIGNALS*

D. C. Lai

Stanford University

Department of Electrical Engineering
Stanford, California 94305

R. L. Lux

University of Utah Medical Center

Cardiology Division
Salt Lake City, Utah 84112

INDEX TERMS - EEG, Frequency discrimination, Narrow-band process, Entrainment of EEG alpha rhythm, Computer analysis.

I. INTRODUCTION

The experimental analysis of EEG waveforms has been dominated by spectral decomposition and amplitude analysis, mainly autocorrelogram techniques though crosscorrelation technique has been used for phase measurements. These techniques as applied to the analysis of EEG signals are abundant in literature. To cite a few of them, we note that the earliest ones were done by Brazier and Barlow [1], [2], [3], [4], and notable simplifications done by Kamp, et al. [5], DeBoer and Kuyper [6], and Vo-Ngoc et al [7]. The fact that the phases of EEG signals as compared to a reference clock signal contain information about the mental alertness has been pointed out to us by Anliker [8] who has used phase-vector and contour-graphic techniques to study the phase entrainment phenomenon. Adey and Walter [9] have used a phase detection technique in the analysis of EEG records in the cat. The EEG α-rhythm has been treated as the result of mutual synchronization of a population of spontaneously oscillatory processes by Wiener [10]. The potential usefulness of the phase entrainment in either recognizing the pathological states of the brain or classifying mental states might be widely explored if investigators had a reliably simple direct measurement technique. In this paper we describe a frequency discrimination technique as realized by an inexpensive frequency discriminator for direct on-line measurement of the entrainment phenomenon in EEG as entrained by the frequency of a sensory stimulus. We demonstrate the use of this device for detecting the presence or absence of the stimulus effect and the measurement of the time delays in the entrainment.

In our study, the EEG signal is first filtered by a narrow-band filter with center frequency about the α-rhythm of the individual. We shall denote this filtered EEG signal as alpha signal $\alpha(t)$. It is then reasonable to consider the alpha signal as narrow-band random process with the alpha frequency f_α as the mean frequency of the spectral band. Then a sample function of this random process is expressed as [11]

$$\alpha(t) = a(t) \cos [2\pi f_\alpha t + \phi(t)] \qquad (1)$$

If the bandwidth of its power density spectrum is much smaller than its mean frequency f_α, then the processes $a(t)$ and $\phi(t)$ in Equation (1) will be slowly varying functions of time as compared to $\cos 2\pi f_\alpha t$ so that the interpretation of $a(t)$ and $\phi(t)$ as envelope and phase has meaning. The alpha signal process $\alpha(t)$ can thus be interpreted as amplitude and phase modulated signal process with carrier frequency f_α. The process $\phi(t)$ can also be interpreted as a relative phase angle, in the sense that the alpha signal process $\alpha(t)$ differs in phase from the signal $(\cos 2\pi f_\alpha t)$ by $\phi(t)$. It is only in this manner that we are able to ascribe meaning to the phase of EEG as a time-varying quantity. The fact that the angular velocity or frequency in radians per second is the time derivative of the angular position leads us to define the instantaneous frequency $f_i(t)$ in cycles per second or Hertz by

$$f_i(t) = f_\alpha + \frac{1}{2\pi}\frac{d\phi}{dt} \qquad (2)$$

The second term in Equation (2) which is proportional to the rate of change of the time-varying phase $\phi(t)$ can be interpreted as the instantaneous frequency deviation relative to the α frequency f_α provided it is stable. Our technique to be described in detail provides a direct measurement of $(d\phi)/(dt)$. The study on the statistical properties of the random processes $a(t)$ and $\phi(t)$ will be reported in another article.

When the brain is excited by an outside stimulus frequency f_s and the EEG is entrained by the stimulus, then we should have

$$f_i(t) = f_\alpha = f_s, \quad t_n + \tau_n \le t \le t_f + \tau_f \qquad (3)$$

where t_n and t_f signify respectively the time instants at which the stimulus is on and the stimulus is off, and τ_n denotes the time delay between t_n and the time instant at which the entrainment occurs and τ_f, the time delay between t_f and the time instant at which the entrainment disappears. Equation (3) implies that

$$\frac{d\phi}{dt} = 0, \quad t_n + \tau_n \le t \le t_f + \tau_f \qquad (4)$$

Since our technique measures $(d\phi)/(dt)$ directly, the measurement of EEG signals which were recorded while the human subjects with eyes closed were stimulated by stroboscopic flashes at the rate of 10 flashes per second for one minute, then no stimulation for one minute, then another minute of stimulation, etc., does show that $(d\phi)/(dt) = 0$ for alternate one minute intervals.

The schemes used for the measurement of $(d\phi)/(dt)$, τ_n, and τ_f, and for the automatic detection of the states of stimulus-on and stimulus-off in the EEG are to be described next.

II. METHOD

An ideal frequency discriminator should produce an output voltage linearly dependent on input

*A portion of this work was carried out at the Department of Electrical Engineering of the University of Vermont, Burlington, Vermont, and was supported in part by NASA Grant NGR 46-001-038. It was also supported in part by NASA Grant NGR 05-020-575 and ARPA Contract DAHC 15-72-C-0232 at Stanford University.

frequency. There are many ways for the realization of frequency discrimination. The most commonly used one is the so-called balanced demodulator with the well-known S curve. The scheme which we have used here is the zero-crossing detector type as described in [12]. In order to eliminate the influence of the amplitude variation $a(t)$, we use an amplifier followed by a hard limiter in front of the detector. The output of the frequency discriminator is proportional to the instantaneous frequency $f_i(t)$ as expressed in Equation (2), and does not depend on the amplitude of the signal. We are, however, interested in the rate of change of $\phi(t)$. The value f_α in Equation (2) is subtracted. In our device f_α can be preset at any value in the range of 5-15 Hz. The device thus yields $(K/2\pi)(d\phi/dt)$ on-line. The characteristic curve of the device is given in Fig.1. In Fig. 2, we show the functional block diagram of the analysis scheme. Detailed circuitry of the device is given in Fig. 3.

The response time or delay τ_n (or τ_f) is defined as the length of time elapsed since the onset (or end) of stimulus to the time instant at which the brain wave is entrained (or desynchronized). This delay τ_n (or τ_f) is, in a sense, the time which the brain takes to synchronize (or desynchronize). There is a noticeable delay between the onset of stimulus-on (or stimulus-off) and the time at which the entrainment is measurable. This fact is shown in Fig. 4 where the $(d\phi)/(dt)$ as the output of the frequency discriminator does not reach a flat plateau (or start to wander) immediately after the onset of stimulus-on (or stimulus-off). The fluctuation of the $x(t) \triangleq (d\phi)/(dt)$ curve is measured by the quantity

$$\rho \triangleq \sum_{i=1}^{N} |x(t_i) - m_N| \qquad (5)$$

within a specified window width N, where m_N is the mean value of $(d\phi)/(dt)$ or $x(t)$ in the window; i.e.,

$$m_N = \frac{1}{N} \sum_{i=1}^{N} x(t_i) \qquad (6)$$

New values of ρ are calculated by sliding the window. The onset of the flatness (or the wandering) is determined by the time instant at which ρ is below (or above) a preset threshold that is determined experimentally. The response time or delay τ_n (or τ_f) is measured as the time lapse between the onset of stimulus-on (or stimulus-off) and the onset of the flatness (or the wandering) of $(d\phi)/(dt)$ as measured by ρ. Owing to the delay introduced by the window width, a correction constant is subtracted from the above obtained time intervals.

The detection scheme utilizes the same program as that used in measuring the response time or delay, but without the prior knowledge of the onset of stimulus-on and stimulus-off. In other words, the influence of stimulus (entrainment) is said to be detected whenever the quantity ρ reaches a value below a preset threshold.

These schemes are realized by digital computer programs in PAL III language used on a PDP-8 computer. Both of these measurements can be performed on-line. Figure 5 depicts the flow chart of the computer program for the response-time measurement.

III. RESULTS

Although the measurements were performed on EEG signals recorded on magnetic tape, they can be performed on-line. As mentioned before, these EEG signals were recorded while the subjects with eyes closed were stimulated by stroboscopic flashes for one minute at the rate of 10 flashes per second, then no stimulation for one minute, then another minute of stimulation, etc. The flashes were generated by Grass photo stimulator model PS-2E on its intensity scale No. 2. The EEG signals are the differential potentials between the electrodes placed at left parietal and left occipital. The EEG signals are referred to as either stimulus-entrained or non-entrained. In order that the EEG signal be more appropriately described by the narrow-band-process model, the EEG signal was passed through a narrow-band filter with a band-width of 1.5 Hz centered at 10 Hz to obtain the alpha signal $\alpha(t)$ as described previously.

A section of the output of the frequency discriminator along with the same section of EEG signals of subject B being analyzed and a square wave indicating when the stimulus was turned on or off are shown in Figs. 6 and 7. The display of apparent high frequency components in the raw EEG of Figs. 6 and 7 are due to the slower writing speed (30 cm per minute) of our strip chart recorder as compared to the conventional writing speed. It is clearly seen that there is a delay following the onset of the stimulus before entrainment is detected; the EEG remains synchronized for a short period of time also after the stimulus was turned off. In Figs. 8, 9, and 10, we show the output of the frequency discriminator with the early, middle, and late sections of EEG signals of subject H as the input along with a square wave indicating the events of stimulus-on and stimulus-off. The offset of time coordinates in the above figures is due to the positions of pens of the strip chart recorder. From these figures, we observe that subject H synchronized with the stimulus very well at the beginning section (13th min. to 19th min.) of the experiment as shown by the measurement of $(d\phi)/(dt)$ depicted in Fig. 8. As shown in Fig. 9, however, the subject's EEG signal did not entrain to the stimulus frequency as well during the middle (105th min. to 111th min.) of an experimental session which lasted about three hours. There is no sign of entrainment of the EEG signal in the end section (176th min. to 182nd min.) of the experiment as shown in Fig. 10. The capability to synchronize with the stimulus may be a measure of certain brain states such as alertness. Further study is needed for this measurement by this technique. The frequency discrimination technique as realized by an inexpensive device is effective in measuring the entrainment phenomenon of EEG signals.

It is possible that variations in the delays τ_n and τ_f in synchronization and desynchronization, respectively, might give some indication of change of levels of alertness, although our data does not include alertness estimates. Results of the measurement of delays for both subjects are shown in Figs. 11 and 12, respectively. The abscissas in the figures denote the time since the beginning of the experiments and the ordinates are the measured delays. Any $\tau_n > 25$ seconds is considered as not synchronized. Subject B seems to have longer response time to stimulus-on in the first hour of experiment than those in the second hour. Subject H did not entrain so well after the first hour of experiment. In general, we see that it takes longer for the subjects to synchronize with the stimuli than it takes to return to the natural states after the stimuli were shut off. The statistics of τ_n and τ_f and their correlation with the mental

states of subjects need further study. However, the technique for measuring these delays is satisfactory.

In Figure 13, we show a typical section of the conditions or states of the stimulus-on and stimulus-off of EEG as results of computer analysis of the output of the frequency discriminator in comparison with the timing track for the on and off of the stimulus. This was generated by a double-threshold detector. The thresholds were determined experimentally. We analyzed the records of both subject B and subject H. The ratio of the sum of the differences between the time of the on and off conditions of EEG as determined by the detector and on-off timing track for the stimulus to the total time of on and off as measured by the timing track was calculated. This ratio is 28.6 per cent for subject B and 35.8 per cent for subject H. We did not take into account the time delays introduced by the smoothing window and the frequency discriminator in the evaluation of these ratios. The values of these ratios may be reduced. The use of the above-mentioned ratio as a performance measure of the detector is appropriate if we do not have the knowledge of the length of time and the manner in which the stimulus is turned on or off. With the knowledge that the stimulus was turned on for one minute, then shut off for one minute, then was on for another minute, etc., and counting only the number of the on-off cycles as determined by the detector, we obtain the following result:
(1) For subject B, there are 57 on-off cycles detected by the detector as compared to 57 on-off cycles on the timing track (a 100 per cent detection).
(2) For subject H, there are 56 on-off cycles detected by the detector as compared to 59 on-off cycles on the timing track (a 94.7 per cent detection).

IV. CONCLUSIONS

The frequency discrimination technique described here has been effective in measuring the entrainment phenomenon in EEG signals. We have shown that the narrow-band-process model used here for characterizing signals is valid. The technique as realized by an inexpensive device described previously provides an effective way for further study on the synchronization phenomenon as related to alertness. Statistical properties of the phase $\phi(t)$ must be gathered for further interpretation of mental states.

V. ACKNOWLEDGEMENT

The authors wish to thank Dr. J. E. Anliker of NASA-Ames Research Center for furnishing the EEG data used in this study, and for many valuable suggestions.

REFERENCES

1. M.A.B. Brazier, Crosscorrelation and Autocorrelation Studies of Electroencephalographic Potentials, Electroenceph. Clin. Neurophysiol., 1952, 4:201.
2. M.A.B. Brazier and J.S. Barlow, Correlation Analysis of Brain Potentials, Electroenceph. Clin. Neurophysiol., 1955, 7:463.
3. J.S. Barlow, et al., The Application of Autocorrelation Analysis to Electroencephalography, Proc. of the First National Biophysics Conf., Yale Univ. Press, New Haven, 1959, 622p.
4. J.S. Barlow, Auto-correlation and Cross-correlation Analysis in Electroencephalography, IRE Trans. on Med. Electron., 1959, ME-6: 179-183.
5. A. Kamp, W. Storm Van Leeuwen and A.M. Tielen, A Method for Auto- and Cross-relation Analysis of the EEG, Electroenceph. Clin. Neurophysiol., 1965, 19:91-95.
6. E. DeBaer and P. Kuyper, Triggered Correlation, IEEE Trans. on Bio-Med. Engineering, 1968, BME-15:169-179.
7. B. Vo-Ngoc, et al., A Possible Procedure to Calculate Correlation Functions for the EEG (Correspondence), IEEE Trans. on Bio-Med. Engineering, 1970, BME-17:265-267.
8. J.E. Anliker, Private Communication 1968.
9. W.R. Adey and D.O. Walter, Application of Phase Detection and Averaging Techniques in Computer Analysis of EEG Records in the Cat, Experimental Neurology, 1963, 7:186-209.
10. N. Wiener, Nonlinear Problems in Random Theory, M.I.T. Press, Cambridge, Mass., 1958, 67-77.
11. W.B. Davenport, Jr., and W.L. Root, An Intro. to the Theory of Random Signals and Noise, McGraw Hill, N.Y., 1958, 158 p.
12. M. Schwartz, Information Transmission, Modulation, and Noise, Second Ed., McGraw Hill, N.Y., 1970, 261-263.

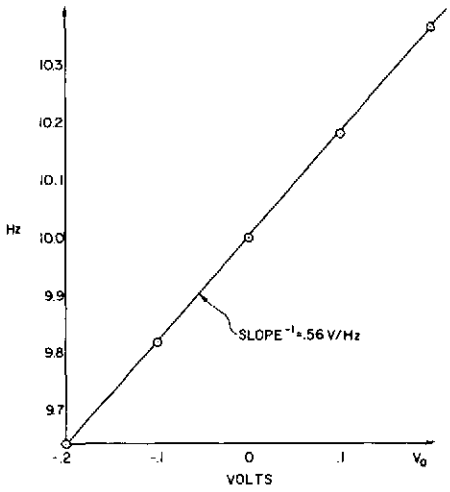

FIG. 1 FREQUENCY DISCRIMINATOR OUTPUT CHARACTERISTIC.

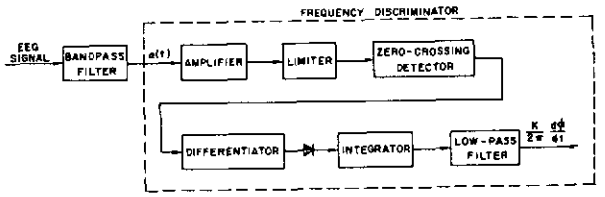

FIG. 2 BLOCK DIAGRAM OF THE ANALYSIS SCHEME.

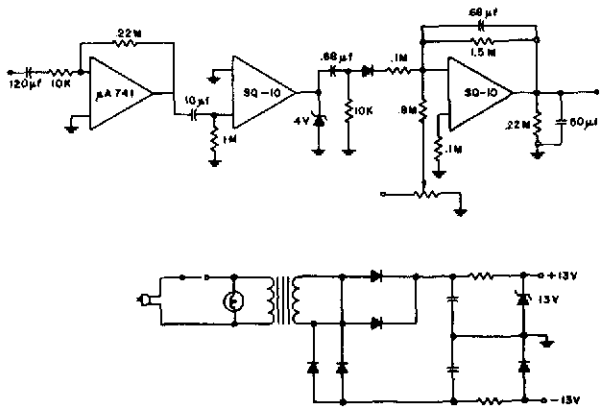

FIG. 3 FREQUENCY DISCRIMINATOR - CIRCUIT DIAGRAM.

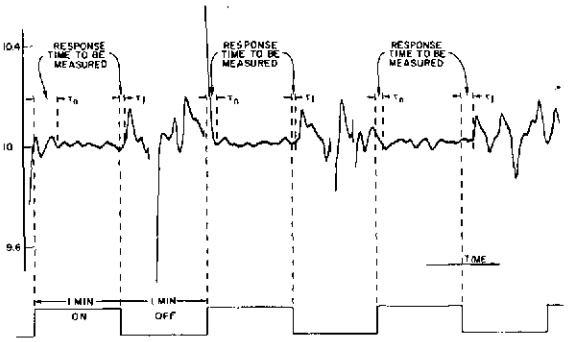

FIG. 4 RESPONSE TIME OR DELAY MEASURED.

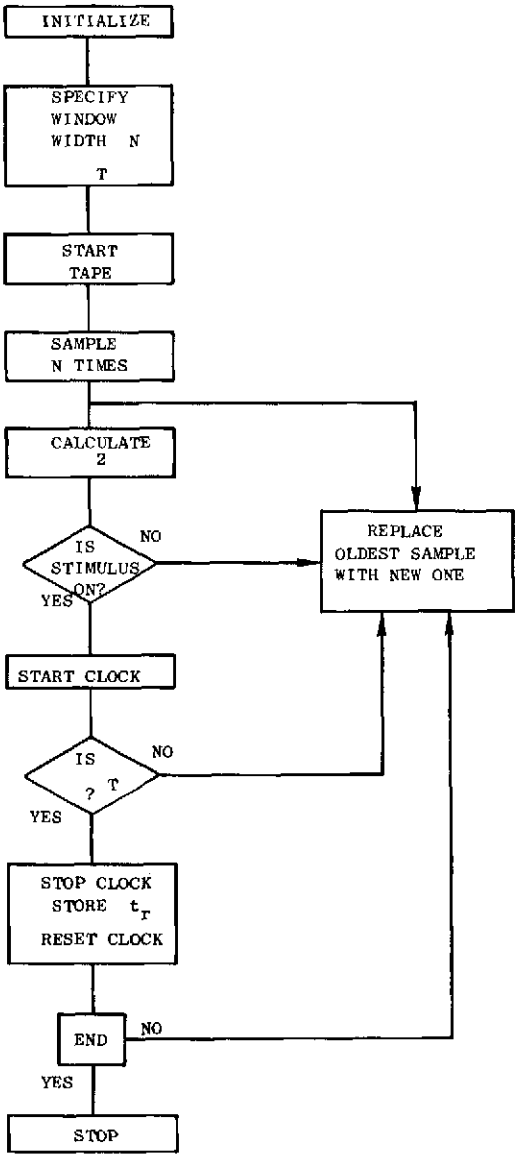

FIG. 5 FLOW CHART FOR THE RESPONSE-TIME MEASUREMENT PROGRAM.

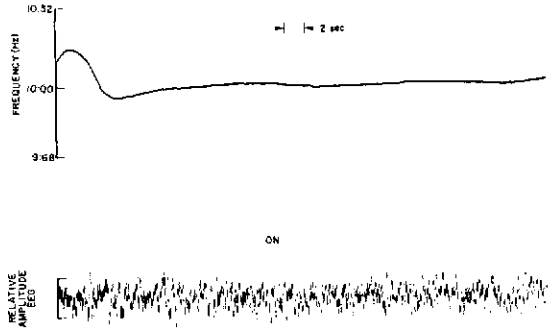

FIG. 6 MEASUREMENT OF $\frac{d\phi}{dt}$ AND THE DISPLAY OF RAW EEG INPUT TO THE SCHEMATIC DIAGRAM SHOWN IN FIG. 2 WHEN STIMULUS IS ON. STRIP-CHART RECORDER WRITING SPEED IS 30 CM PER MINUTE.

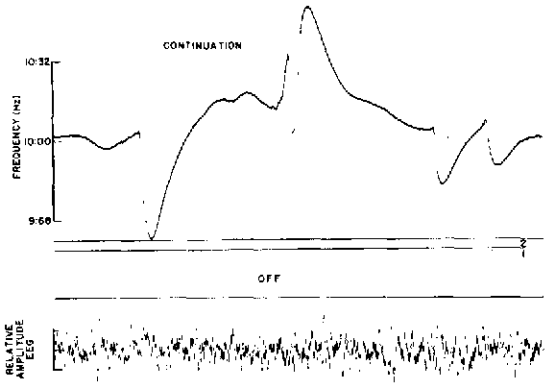

FIG. 7 MEASUREMENT OF $\frac{d\phi}{dt}$ AND THE DISPLAY OF RAW EEG INPUT TO THE SCHEMATIC DIAGRAM SHOWN IN FIG. 2 WHEN STIMULUS IS OFF. STRIP-CHART RECORDER WRITING SPEED IS 30 CM PER MINUTE.

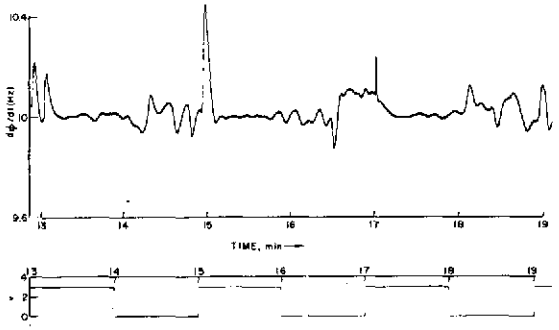

FIG. 8 MEASUREMENT OF $\frac{d\phi}{dt}$ OF THE ALPHA SIGNAL OF THE EARLY PART OF EEG RECORD OF SUBJECT H.

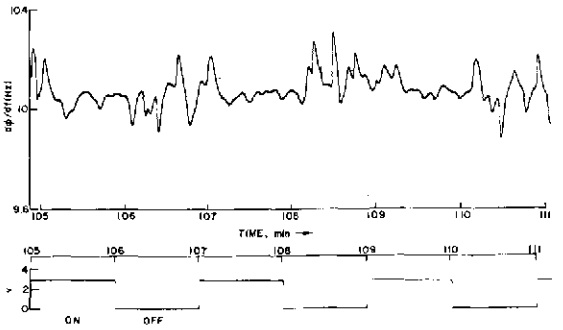

FIG. 9 MEASUREMENT OF $\frac{d\phi}{dt}$ OF THE ALPHA SIGNAL OF THE MIDDLE PART OF EEG RECORD OF SUBJECT H.

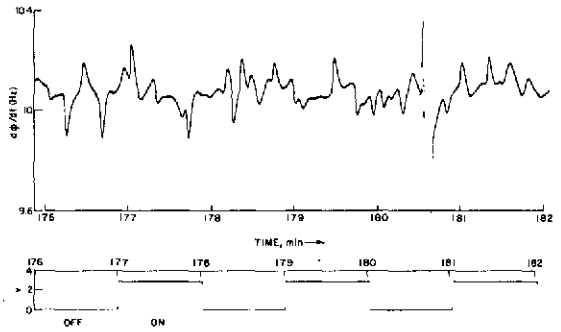

FIG. 10 MEASUREMENT OF $\frac{d\phi}{dt}$ OF THE ALPHA SIGNAL OF THE LATE PART OF EEG RECORD OF SUBJECT H.

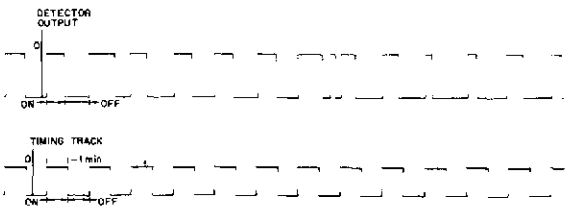

FIG. 13 THE STATES OF STIMULUS-ON AND STIMULUS-OFF OF EEG AS RESULTS OF THE ANALYSIS IN COMPARISON WITH THE ACTUAL ON AND OFF OF THE STIMULUS.

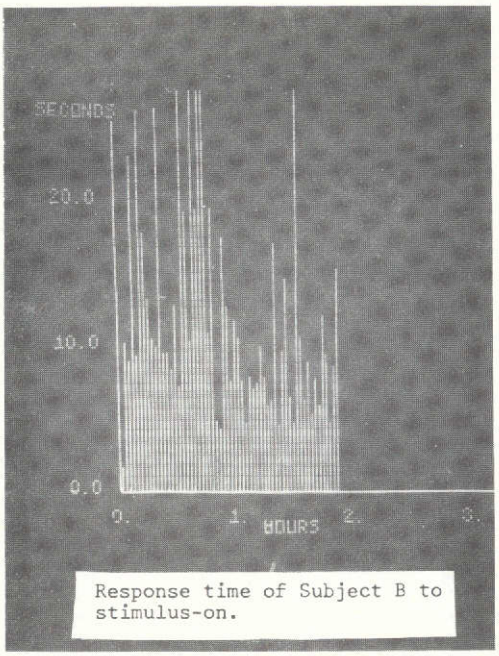

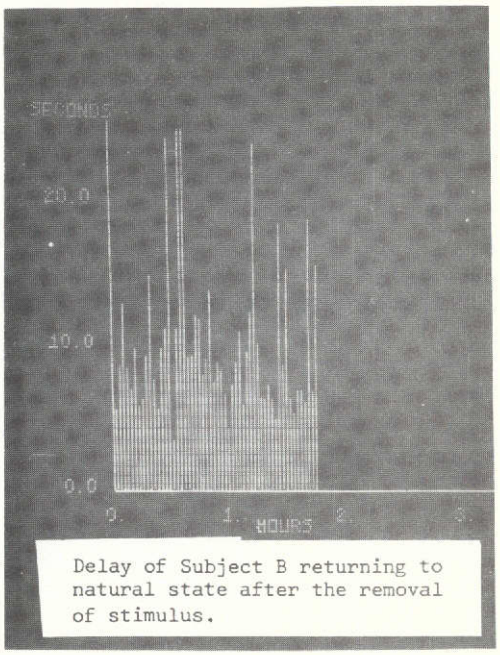

Fig. 11. RESPONSE TIME STUDY OF SUBJECT B.

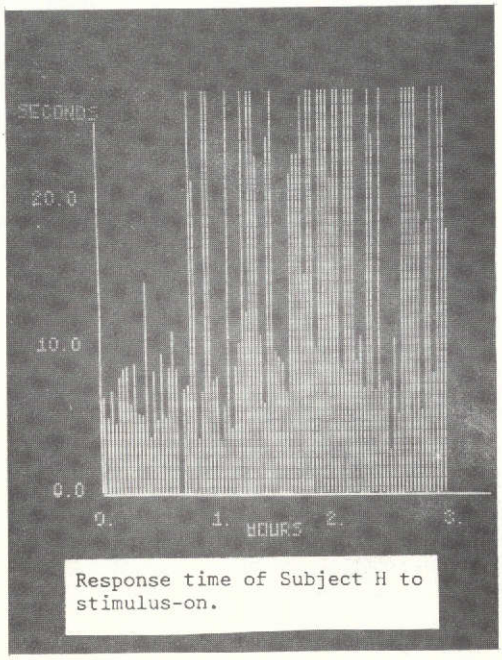

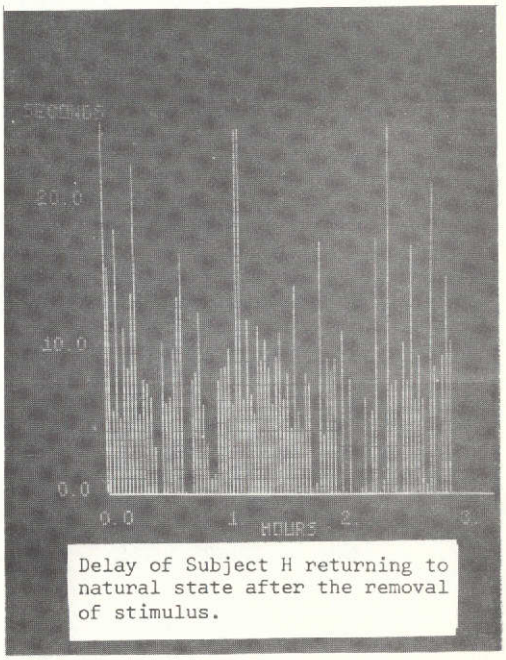

Fig. 12. RESPONSE TIME STUDY OF SUBJECT H.

M. Ein-Gal and D.C. Lai

In the study of brain functions or monitoring patients in clinical laboratory, a non-invasive scheme for monitoring either psycho-physiological states or pathological states via the analysis of EEG signals is an important tool. In view of the time-varying nature of these states, we are interested in monitoring them on a moment-by-moment basis. To this aim, we have devised a digital scheme which is capable of tracking the amplitude, frequency, and phase of a particular EEG rhythm in real time. The amplitude, frequency, and phase are assumed to be low-pass process. These 3-tuples may be treated as a 3-dimensional vector whose trajectories in the 3-space relate to the change of psycho-physiological states or pathological states. This scheme is implemented on a PDP-15 computer system. We characterize EEG $e(t)$ as a narrowband process, hence

$$e(t) = a(t) \cos \theta(t) = a(t) \cos [\omega_o t + \varphi(t)] ,$$

or $$e(t) = c(t) \cos \omega_o t + s(t) \sin \omega_o t .$$

By tracking the center frequency ω_o, we may decompose the signal into two components; viz., the in-phase component $c(t)$ and the quadrature component $s(t)$. A digital system depicted in Fig. 1 tracks the center frequency ω_o and resolves the input EEG waveform into $c(t)$ and $s(t)$. This system is composed of three major components:

(a) Voltage-controlled oscillators and amplitude regulator,
(b) Frequency discriminator,
and (c) Low pass filters.

The VCO is realized by a second-order difference equation. The locations of the poles are controlled by the amplitude regulator and by the frequency discriminator. The realization of the frequency discriminator is obtained by averaging the rate of change of phase over a preselected interval in accordance with the desired time constant of the loop. Applying $c(t)$ and $s(t)$ to the horizontal and vertical axes respectively, we obtain a two-dimensional trajectorial plot where the envelope $a(t)$ and the phase $\varphi(t)$ are proportional to the radius and angle respectively in the polar coordinate system.

As an example, this real-time monitoring technique was applied to the EEG data obtained while the subjects with eyes closed were stimulated by stroboscopic flashes for one minute at the rate of 10 flashes per second, then no stimulation for one minute, then another minute of stimulation, etc. The flashes were generated by Grass photo stimulator model PS-2E on its intensity scale no. 2. The EEG signals are the differential potentials between the electrodes placed at left parietal and left occipital. The results are shown in Figures 2 and 3. Figure 2 depicts the representation of EEG when stimulus was off by using this scheme. Figure 3 shows the representation of EEG when stimulus was on. The plots in both figures are normalized with respect to certain scale for visual convenience and they are plotted simultaneously. The top one is the trajectorial plot of the envelope $a(t)$ and phase $\varphi(t)$ in polar coordinates. The second one is the plot of frequency versus time. The third and forth are the rate of change of amplitude and phase, respectively. The fifth and the sixth are the phase $\varphi(t)$ and amplitude $a(t)$, respectively, The seventh is the EEG signal analyzed. The last is the output of VCO which is used as reference. Notice that the frequency and the phase are practically constant when stimulus was on.

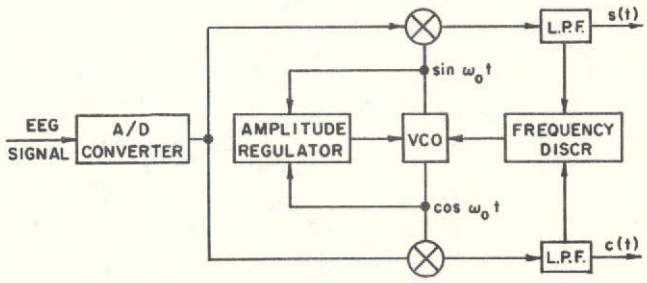

Figure 1. Resolver of in-phase and quadrature signals

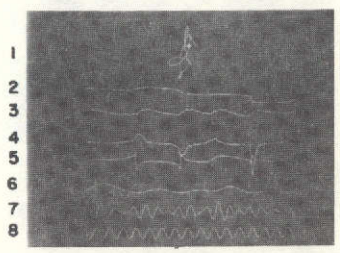

Figure 2. Representation of stimulus-off EEG signal

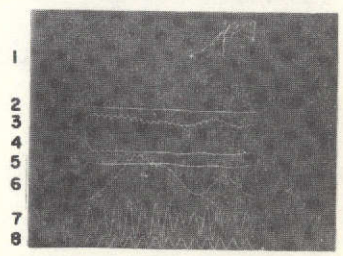

Figure 3. Representation of stimulus-on EEG signal

This work was supported in part by the Advanced Research Projects Agency of the Department of Defense under Contract DAHC15-72-C-0232 and NASA under Grant NGR-05-020-575.

Stanford University
Department of Electrical Engineering
Stanford, California 94305

ERROR-FREE EEG SIGNAL REPRESENTATION

M. Ein-Gal and D. C. Lai

Stanford Electronics Laboratories
Stanford University
Stanford, California 94305

Summary

The representation of electroencephalographic signals is an important problem for real-time monitoring of either psycho-physiological states or pathological states. A representation of any EEG rhythm in its in-phase and quadrature components is given. This representation gives zero error when the signal is reconstituted from its representatives. Derivation of the scheme is reported. Using this scheme, a digital real-time system for obtaining this representation is designed and realized by a PDP-15 computer. An example with a typical EEG signal as the input to the system is included to demonstrate the accuracy of the representation.

I. Introduction

A digital real-time system is described for obtaining the representation of a particular EEG rhythm in its in-phase and quadrature components with the constraint that the error is zero when synthesized. In a way, this system provides a form of data compression. The resultant representation can be advantageously employed for data transmission and data storage as well as real-time monitoring of either psycho-physiological states or pathological states. For these applications, the requirement of an error-free synthesis or reproduction of the EEG signal is imperative.

A common scheme for obtaining the in-phase and quadrature components of a signal is to multiply the signal by an oscillator outputs at quadrature with the center frequency f_o of the signal and then passing the resultants through low-pass filters in the forward path. However, this method does not provide a faithful replica of the signal when the two components are synthesized. The error arises mainly from the phase distortions of the filter or the pure delays of the non-recursive filter. Our digital system uses, instead, an oscillator running at twice the center frequency of the signal and a filter in the feedback path. This filter does not affect the reproduction fidelity; however, it plays a role in determining certain statistical properties of the slowly varying components of the resultant representatives. Hence, one may choose a filter to minimize certain properties of the outcome such as the bandwidth, variance, etc.

II. Derivation of the Scheme

Let the input signal in its digitized form be $y(N)$. We shall define a two-dimensional oscillator vector $H(N)$ by

$$H^T(N) \triangleq \left[\cos 2\pi f_o N \quad \sin 2\pi f_o N\right]. \tag{1}$$

We may write

$$y(N) = X^T(N)H(N) \tag{2}$$

where $X(N)$ is a two-dimensional vector whose components $x_1(N)$ and $x_2(N)$ are the slowly-varying components sought after. Note that the Equation (2) is not unique since there exist many $X(N)$ which could satisfy (2). For certain particular choice, $x_1(N)$ and $x_2(N)$ are related by Hilbert transform. Let $\hat{X}(N|N-1)$ be a function of the past values of $X(N)$. For instance, $\hat{X}(N|N-1)$ could be a linear combination of $X(0)$, $X(1)$, ..., $X(N-1)$. Denote the difference between $X(N)$ and its $\hat{X}(N|N-1)$ by

$$E(N) = X(N) - X(N|N-1) . \tag{3}$$

The norm of the difference is

$$\|E(N)\| = \left[E^T(N)E(N)\right]^{1/2} . \tag{4}$$

We choose $X(N)$ by minimizing (4) but satisfying (2) simultaneously. The solution thus obtained is

$$X(N) = \tfrac{1}{2}\left[I - A(N)\right] \hat{X}(N|N-1) + H(N)y(N) \tag{5}$$

where I is the identity matrix and $A(N)$ is the matrix with its components given by the double-frequency oscillator; i.e.,

$$A(N) = \begin{bmatrix} \cos 4\pi f_o N & \sin 4\pi f_o N \\ \sin 4\pi f_o N & -\cos 4\pi f_o N \end{bmatrix}. \tag{6}$$

If $\hat{X}(N|N-1)$ is the best linear estimator of $X(N)$ based on its past history, then the representation of the input signal $y(N)$ by the vector $E(N)$ corresponds to the innovation representation $\nu(N)$ with

$$\overline{\|E(N)\|^2} = \overline{\nu^2(N)} \tag{7}$$

where $\nu(N) = y(N) - \hat{y}(N|N-1)$ and $\hat{y}(N|N-1)$ is the best linear estimator of $y(N)$ in terms of its past values $y(0)$, $y(1)$, ..., $y(N-1)$.

III. Results and Conclusions

The digital system is depicted by a block diagram shown in Figure 1. The oscillator is realized by a second order difference equation whose coefficients are controlled by the amplitude regulator and the output of the frequency discriminator. As a demonstration, we select a typical EEG signal as the input waveform to our digital system. We show both the original EEG signal and the synthesized EEG signal from these two components in Figure 2. Note the high fidelity of the reproduction. The filter in the feedback path was chosen to minimize the first order difference $\|X(N) - X(N-1)\|$. The EEG data were furnished by Dr. J. E. Anliker of NASA-Ames Research Center.

This work was supported in part by the Advanced Research Projects Agency of the Department of Defense under Contract DAHC 15-72-C-0232 and NASA under Grant NGR-05-020-575.

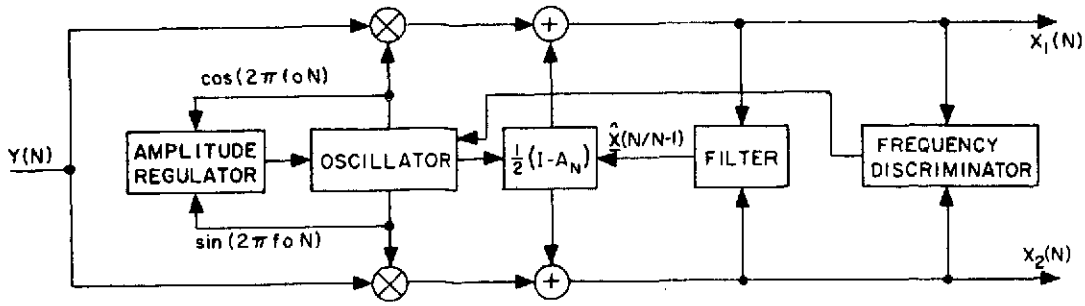

Figure 1 Block diagram of the digital system for resolving the signal into in-phase and quadrature components.

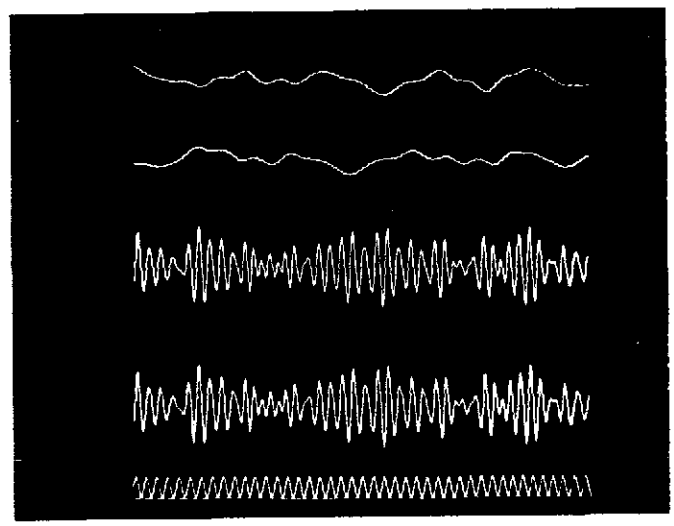

Figure 2 Representation of EEG Signal

1. $x_1(N)$, the in-phase component.
2. $x_2(N)$, the quadrature component.
3. The original EEG signal.
4. The reproduced EEG signal synthesized from x_1 and x_2.
5. The reference signal.

Reprinted by permission from 1973 IEEE PROCEEDINGS OF THE INTERNATIONAL CONFERENCE ON CYBERNETICS AND SOCIETY
Catalogue No. 73CHO799-7SMC, pp. 242-243

ESTIMATING SIGNAL AND NOISE IN COHERENT TIME AVERAGES OF EEG DATA

James Anliker, Ph.D.; David Lai, Ph.D.*; Tamara Rimmer, B.S.;
and Herbert Finger, M.S.E.E.
NASA-Ames Research Center, Moffett Field, California 94035

Coherent time averaging is widely used in the study of evoked responses as a technique for extracting coherent signals from incoherent noise. This paper is concerned with the problem of estimating, in real time, the signal and noise components in coherent time averages of sample functions of EEG alpha activity in the presence and in the absence of coherent trains of photic stimuli.

The rationale for using a coherent time averaging algorithm in the study of evoked potentials is well known and seemingly straight-forward: events in each sample function that are coherent with the time base of the averager (i.e., bear a consistent temporal relationship to the trigger) will be enhanced by averaging (or summing) whereas incoherent or random events will tend to cancel out. The implication is that when a small signal is mixed with a lot of noise, the signal can be extracted by averaging a sufficiently large number of sample functions. However, in the case of electrophysiological potentials, neither the signal characteristics nor the signal-to-noise ratio is known; consequently, it is not clear how to select the best number of sample functions to include in the ensemble average. It is also unfortunate that the probability that a physiological process will remain stationary throughout the averaging time decreases as the averaging time increases. Thus, in an attempt to compensate for a low signal-to-noise ratio by increasing the number of sample functions in the average, the experimenter may be thwarted by significant non-stationarity. Similarly, from a control theoretical point of view, the experimenter is in a double bind: a compromise must be reached between the desire to avoid decisions based on insufficient data and the conflicting desire to maintain the shortest possible feedback loop. We have sought to minimize these problems by developing a real time signal-to-noise estimation algorithm.

We have used a LINC-8 computer for implementation of our estimation scheme and for analyzing the coherent changes in the EEG alpha rhythm in response to coherent trains of 10 microsec photic flashes (Grass PS-2 photostimulator at intensity #4) delivered through closed eyelids. The interflash period was set equal to the mean period of the autonomous alpha rhythm as measured by autocorrelation. Individual right and left occipital scalp electrodes were referred to the yoked earlobe electrodes. The cortical potentials were amplified, filtered (bandpass=5 Hz with 24 db per octave roll-off), and converted into digital form at a 1 msec sampling rate. Each sample function was 175 msec duration and was always synchronous with a flash at T_0. The average amplitude of the detected peaks was measured. This value was treated as the maximum signal contribution to the average to be expected if the signal were fully coherent. The discrepancy between the coherent prediction and the obtained average was treated as noise. The ratio of signal to the combined signal and noise estimates was re-computed as each new sample function was entered into the average. An analog voltage proportional to this ratio was immediately output and displayed on a storage oscilloscope. Figure 1 shows the superimposed

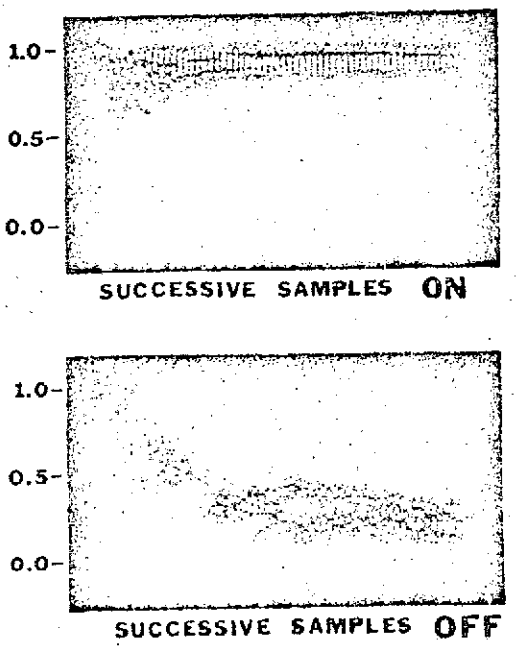

FIGURE 1. Signal /(Signal + Noise) Ratios

successive ratio values for seven 58-sample function averages of stimulus-ON (top) and the same number of sample functions for the stimulus-OFF condition (bottom). The successive ratios for a single cumulative average constitute a sort of "stabilization pathway" for the average. It is readily apparent in these records that there is greater redundancy as the number of sample functions in the average increases, and that there is a large difference between the stimulus-ON and stimulus-OFF conditions. Consequently, we believe that this estimation scheme holds considerable potential for quantitative, fully automatic assessments of signal and noise components in this type of evoked response.

The authors wish to acknowledge the technical assistance of Miss Janice McMillin(NASA/ARC).

*Visiting Professor of Electrical Engineering, Stanford University, Stanford, California 94305

Abstracts of the 7th Annual Meeting of THE NEUROELECTRIC SOCIETY
November 20-23, 1974 New Orleans, Louisianna

A NONLINEAR MODEL OF EEG ENTRAINMENT BY PERIODIC PHOTIC STIMULATION

J. R. Nickolls

Stanford University, Stanford, California

D. C. Lai

Stanford University and University of Vermont

J. E. Anliker

NASA/Ames Research Center, Moffett Field, California

The phenomenon that the EEG alpha rhythm synchronizes with periodic visual stimuli has been observed since the beginnings of electroencephalography [1]. The brain's entrainment ability depends on several factors, including its internal state or condition. Since a quantitative estimate of a particular brain state such as alertness has many practical applications, a mathematical model of an associated input-output relationship is of great use. The quantitative variations of the model parameters can be correlated with various brain states using empirical data and model simulation.

We are using a nonlinear oscillator to model a stimulus-response relationship of the brain. In particular, we are investigating the entrainment of the human alpha rhythm by periodic photic stimuli. The model elucidates the relationships between the frequency, phase, and amplitude of the alpha waveform and the frequency and amplitude of the stimulus. This model is clearly applicable to other phenomena such as the flicker effect and photically induced epileptic seizures.

The nonlinear oscillator used in our study is a van der Pol oscillator. This has also been suggested by Dewan [2]. The analysis treats entrainment by pulse trains since our experimental stimuli are stroboscopic flashes. The theoretical analysis is made with an extension of Blaquière's time-domain method [3]. In this paper, we will report on harmonic entrainment, and combined frequency oscillations. Both model-simulated results and extensive experimental results from human subjects will be described and compared.

The simulations of the model have been made on a digital computer, and the results will be presented for direct comparison with results derived from EEG data. The empirical data were obtained from alert subjects photically driven over a wide range of frequencies, and exhibit harmonic,

subharmonic, and superharmonic entrainment, as well as combined frequency oscillations. The model accounts for these critical phenomena well; its validity has been established through extensive empirical EEG data. Further work on the model and its applications are in progress.

References:

1. Walter, W. G.: The Living Brain, New York: W. W. Norton and Company, Inc., 1953

2. Dewan, E. M.: Nonlinear Oscillations and Electroencephalography, J Theor Biology, 7:141-159, 1964

3. Blaquière, A.: Nonlinear System Analysis, New York: Academic Press. 1966

Acknowledgement:

This work was supported in part by the National Aeronautics and Space Administration under Grant NGR-05-020-575 and the Advanced Research Projects Agency of the Department of Defense under Contract DAHC15-72-C-0232 at Stanford University, and in part by NASA under Grant NGR-46-001-041 at the University of Vermont.

Abstract

PREDICTION OF EEG ALPHA WAVEFORMS USING AN AUTOREGRESSIVE MODEL

A. Shah, D. C. Lai, and J. E. Anliker

An autoregressive process X_t of order p is defined by the following difference equation

$$X_t = a_1 X_{t-1} + a_2 X_{t-2} + \ldots + a_p X_{t-p} + e_t$$

where e_t is additive noise and the a's are the parameters of the process. These parameters can be estimated from the time-series by a simple non-iterative least-squares method. For the case where the noise is Gaussian, these least-squares estimates approximate very closely the maximum-likelihood estimates. Such a model is well known for the analysis of stationary time-series. In particular, it has been used quite extensively for the estimation of EEG power spectra. However, the alpha rhythm of the EEG has slowly changing characteristics which can be treated as piece-wise stationary but long samples cannot be treated in this manner. We have developed an algorithm which computes the least-squares estimates of the parameters of a 7th order process from a short sample of the alpha rhythm. The order has been estimated from the autocorrelation and partial autocorrelation functions of the signal. The algorithm then uses the model for least-squares prediction up to some maximum lead time. Probability limits for the forecasts (assuming Gaussian noise) are also computed. As more data becomes available, the sample window is moved forward and the parameter estimates updated to reflect the changing characteristics of the alpha rhythm. The performance of this predictive model is evaluated by the mean-square error in the forecasts. The maximum forecast lead time can be varied. We have found the model quite useful for prediction as much half an alpha cycle (approximately 50 ms.) in advance.